

1 **F-BAR Cdc15 Promotes Gef1-mediated Cdc42 Activation During Cytokinesis and**
2 **Cell Polarization in *S. pombe***

3

4 Brian S. Hercyk and Maitreyi E. Das

5 Department of Biochemistry & Cellular and Molecular Biology, University of Tennessee,
6 Knoxville, TN, USA, 37996.

7

8 **Running title:** Cdc15 promotes Gef1 localization

9

10 **Key words:** Cdc15, Cdc42, Gef1, cytokinesis, polarity

11

12 **Corresponding Author:**

13 Maitreyi Das

14 University of Tennessee, Knoxville

15 415, Ken and Blaire Mossman Building

16 Knoxville, TN, 37996

17 mdas@utk.edu

18 **ABSTRACT**

19 Cdc42, a Rho-family GTPase, is a master regulator of cell polarity. Recently it has been
20 shown that Cdc42 also facilitates proper cytokinesis in the fission yeast,
21 *Schizosaccharomyces pombe*. Cdc42 is activated by two partially redundant GEFs Gef1
22 and Scd1. Although both the GEFs activate Cdc42, their deletion mutants display
23 distinct phenotypes, indicating that they are differentially regulated, by an unknown
24 mechanism. During cytokinesis, Gef1 localizes to the division site and activates Cdc42
25 to initiate ring constriction and septum ingression. Here we report that the F-BAR
26 domain containing Cdc15 promotes Gef1 localization to its functional sites. We show
27 that *cdc15* promotes Gef1 association with the cytokinetic nodes to activate Cdc42
28 during ring assembly. Moreover, *cdc15* phospho-mutants phenocopy polarity
29 phenotypes of *gef1* mutants. In a hypermorphic *cdc15* mutant, Gef1 localizes
30 precociously to the division site, and is readily detected at the cortical patches and the
31 cell cortex. Correspondingly, the hypermorphic *cdc15* mutant shows increased bipolarity
32 during interphase and precocious Cdc42 activation at the division site during
33 cytokinesis. Finally, loss of *gef1* in hypermorphic *cdc15* mutants abrogates the
34 increased bipolarity and precocious Cdc42 activation phenotype. We did not see any
35 change in the localization of the other GEF Scd1 in a Cdc15-dependent manner. Taken
36 together our data indicates that Cdc15 promotes Cdc42 activation specifically via Gef1
37 localization to the division site to facilitate proper cytokinesis and to the cell cortex to
38 promote bipolarity.

39

40 INTRODUCTION

41 The conserved Cdc42 is a master regulator of polarized cell growth in fission yeast
42 (MILLER AND JOHNSON 1994; JOHNSON 1999; ESTRAVIS *et al.* 2012; DAS AND VERDE 2013).
43 Recently, it has also been shown that Cdc42 has a role in cytokinesis, the final step in
44 cell division (WEI *et al.* 2016). Through the regulation of actin and membrane trafficking,
45 Cdc42 controls cellular processes such as growth, cell polarity, and cytokinesis (MARTIN
46 *et al.* 2007; HARRIS AND TEPASS 2010; ESTRAVIS *et al.* 2011; ESTRAVIS *et al.* 2012). Given
47 the complexities of these cellular processes, Cdc42 activation needs to be precisely
48 regulated in a spatiotemporal manner. A prime example of this precise regulation is the
49 oscillation of Cdc42 activation between the two cells ends during bipolar growth (DAS *et al.*
50 *et al.* 2012; DAS AND VERDE 2013). Disrupting Cdc42 activation patterns leads to defects in
51 cell shape and cytokinesis (DAS *et al.* 2012; WEI *et al.* 2016; ONWUBIKO *et al.* 2019).
52 While much is known about how Cdc42 promotes actin organization and polarization,
53 the spatiotemporal manner in which regulation of Cdc42 is fine-tuned is not well
54 understood.

55 Cdc42 is activated by GEFs (guanine nucleotide exchange factors) which exchange
56 GDP for GTP, and inactivated by GAPs (GTPase activating proteins) which enhance
57 the intrinsic rate of GTP hydrolysis (BOS *et al.* 2007). Fission yeasts have two GEFs,
58 Scd1 and Gef1 that control polarization and cytokinesis (CHANG *et al.* 1994; COLL *et al.*
59 2003). While both the GEFs activate Cdc42 and their double deletion is not viable (COLL
60 *et al.* 2003; HIROTA *et al.* 2003), *scd1Δ* and *gef1Δ* mutants exhibit distinct phenotypes,
61 indicating that they differentially activate Cdc42. *scd1Δ* cells are depolarized and exhibit
62 defects in septum morphology (CHANG *et al.* 1994; WEI *et al.* 2016). In contrast, *gef1Δ*
63 mutants exhibit monopolar growth and a delayed onset of ring constriction (COLL *et al.*
64 2003; DAS *et al.* 2015; WEI *et al.* 2016; ONWUBIKO *et al.* 2019). This suggests that the
65 two GEFs allow for distinct Cdc42 activation patterns, which regulate different aspects
66 of cell polarity establishment and cytokinesis. It is unclear how the two Cdc42 GEFs
67 result in distinct phenotypes given they both activate the same GTPase. One potential
68 explanation could be differential regulation of these GEFs. Indeed, during cytokinesis,
69 first Gef1 is recruited to the membrane proximal to the actomyosin ring where it
70 activates Cdc42 to promote timely onset of ring constriction and septum initiation (WEI
71 *et al.* 2016). Next, Scd1 is recruited to the ingressing membrane to promote proper
72 septum maturation (WEI *et al.* 2016).

73 It is unknown what gives rise to the temporal recruitment pattern of the GEFs. How does
74 Gef1, but not Scd1, initially localize to the division site to activate Cdc42 in a timely
75 manner? Gef1 contains an N-BAR domain that is required for its activity but not for its
76 localization (DAS *et al.* 2015). The N-terminal region of Gef1 is necessary and sufficient
77 for its localization (DAS *et al.* 2015). Phosphorylation of the N-terminal region by Orb6
78 kinase generates a 14-3-3 binding site that results in the sequestration of Gef1 in the

79 cytoplasm (DAS *et al.* 2009; DAS *et al.* 2015). While it is known how Gef1 is removed
80 from its site of action, it is unclear what recruits Gef1 to these sites.

81 Here we show that Gef1 localization to its site of action is aided by the F-BAR protein
82 Cdc15. Cdc15 localizes to endocytic patches during interphase and to the division site,
83 where it scaffolds the actomyosin ring (WU *et al.* 2003; ARASADA AND POLLARD 2011;
84 McDONALD *et al.* 2017). We report that Gef1 localizes to cortical nodes at the division
85 site during ring assembly in a *cdc15*-dependent manner. Similarly, we find that *cdc15*
86 promotes Gef1 localization to the cortical patches and cell tips. We show that *cdc15*
87 phospho-mutants phenocopy *gef1* polarity phenotypes. A hypermorphic *cdc15* allele
88 shows precocious Cdc42 activation at the division site during cytokinesis and increased
89 bipolarity during interphase. Finally, we show that enhanced bipolarity and premature
90 Cdc42 activation is abrogated upon deletion of *gef1* in the hypermorphic *cdc15* mutant.
91 This indicates that *cdc15* promotes Cdc42 activation through *gef1*. We did not see any
92 change in the localization of the other GEF Scd1 in a *cdc15*-dependent manner. Taken
93 together our data indicates that Cdc15 specifically promotes Gef1 localization to the
94 division site and the cell cortex to promote Cdc42 activation.

95 **MATERIALS AND METHODS**

96 **Strains and cell culture**

97 The *S. pombe* strains used in this study are listed in Supplemental Table S1. All strains
98 are isogenic to the original strain PN567. Cells were cultured in yeast extract (YE)
99 medium and grown exponentially at 25°C, unless specified otherwise. Standard
100 techniques were used for genetic manipulation and analysis (MORENO *et al.* 1991). Cells
101 were grown exponentially for at least 3 rounds of eight generations before imaging.

102

103 **Microscopy**

104 Cells were imaged at room temperature (23–25°C) with an Olympus IX83 microscope
105 equipped with a VTHawk two-dimensional array laser scanning confocal microscopy
106 system (Visitech International, Sunderland, UK), electron-multiplying charge-coupled
107 device digital camera (Hamamatsu, Hamamatsu City, Japan), and 100×/numerical
108 aperture 1.49 UAPO lens (Olympus, Tokyo, Japan). Images were acquired with
109 MetaMorph (Molecular Devices, Sunnyvale, CA) and analyzed by ImageJ (National
110 Institutes of Health, Bethesda, MD (SCHNEIDER *et al.* 2012)). For still and z-series
111 imaging, the cells were mounted directly on glass slides with a #1.5 coverslip (Fisher
112 Scientific, Waltham, MA) and imaged immediately; fresh slides were prepared every 10
113 minutes. Z-series images were acquired with a depth interval of 0.4 μm. For time-lapse
114 images, the cells were placed in 3.5-mm glass-bottom culture dishes (MatTek, Ashland,
115 MA) and overlaid with YE medium plus 0.6% agar with 100μM ascorbic acid as an
116 antioxidant to minimize toxicity to the cell, as reported previously (FRIGAULT *et al.* 2009;
117 WEI *et al.* 2017).

118

119 **Analysis of fluorescent intensity**

120 Mutants expressing fluorescent proteins were harvested from mid-log phase cultures at
121 OD₍₅₉₅₎ 0.5 and imaged on slides. Depending on the mutant and the fluorophore, 16-18
122 z-planes were collected at a z-interval of 0.4μm for either or both the 488nm and 561nm
123 channels. The respective controls were grown and imaged in an identical manner.
124 ImageJ was used to generate sum projections from the z-series, and to measure the
125 fluorescence intensity of a selected region. The cytoplasmic fluorescence of the same
126 cell was subtracted to generate the normalized intensity. Mean normalized intensity was
127 calculated for each image from all measurable cells (n>5) within each field.

128

129 **Statistical tests**

130 Statistical tests were performed using GraphPad Prism software. When comparing two
131 samples, a student's t-test (two-tailed, unequal variance) was used to determine
132 significance. When comparing three or more samples, one-way ANOVA was used,

133 followed by a Tukey's multiple comparisons post-hoc test to determine individual p-
134 values.

135

136 **Cell staining**

137 To stain the septum and cell wall, cells were stained in YE liquid with 50 µg/ml
138 Calcofluor White M2R (Sigma-Aldrich, St. Louis, MO) at room temperature.

139

140 **Latrunculin A treatment**

141 Cells were treated with 10 µM latrunculin A in dimethyl sulfoxide (DMSO) in YE medium
142 for 30 min before imaging. Control cells were treated with only 0.1% DMSO in YE
143 medium.

144

145 **Analysis of *sin* and *cdc12* mutants**

146 *plo1-25*, *sid2-250*, and control cells were grown in YE at 25°C to OD 0.2, then shifted to
147 the restrictive temperature at 35.5°C. Slides were then prepared and imaged from the
148 cultures at 0, 1, 2, and 4 hour time points. Cells expressing *cdc12ΔC*-GFP were initially
149 grown in EMM (Edinburgh minimal medium) with 150µM Thiamine. Induction of
150 *cdc12ΔC*-GFP expression was performed as described previously (YONETANI AND
151 CHANG 2010). Briefly, cultures were harvested by low speed centrifugation, rinsed, and
152 then grown in EMM without thiamine for 18 hours prior to imaging.

153

154 RESULTS

155 **Gef1 localizes to cytokinetic nodes**

156 While we have previously characterized the distinct localization pattern and phenotypes
157 of the Cdc42 GEFs, Gef1 and Scd1 during cytokinesis (WEI *et al.* 2016), how they are
158 recruited to the division site at the appropriate time is unknown. Since Gef1 is
159 detectable at the membrane proximal to the assembled actomyosin ring, we posited that
160 the ring is required for Gef1 localization. To test this, we treated cells with 10 μ M
161 Latrunculin A (LatA) for 30 min to depolymerize actin structures, then observed the
162 localization of Gef1-mNeonGreen (Gef1-mNG). Gef1-mNG localizes to the membrane
163 proximal to the actomyosin ring, marked by Rlc1-tdTomato, in mock DMSO treated cells
164 (Fig. 1A). Rlc1-tdTomato rings fragment upon treatment with LatA, as does Gef1-mNG,
165 indicating that an intact ring is necessary for proper Gef1 localization. We observe that
166 upon LatA treatment, Gef1-mNG does not diffuse away into the cytosol, but instead
167 localizes to cortical nodes about the cortex with Rlc1-tdTomato. Upon closer
168 examination of these nodes, one population of Gef1 can be seen to partially colocalize
169 with Rlc1, while the other population of Gef1 puncta do not overlap with Rlc1 (Fig. B).
170 These findings indicate that Gef1 may interact with or be recruited by one of the
171 proteins within these cortical nodes.

172 Since Gef1 promotes timely onset of ring constriction (WEI *et al.* 2016), we asked if Gef1
173 localization itself was under a temporal control during cytokinesis. Given that Gef1
174 arrives at the division site during anaphase as the actomyosin ring assembles (WEI *et*
175 *al.* 2016), we asked whether Gef1 is recruited in a cell cycle-dependent manner. To test
176 this, we induced ectopic ring formation in interphase cells using the constitutively active
177 formin mutant, *cdc12 Δ C*-GFP (YONETANI AND CHANG 2010). In the presence of thiamine,
178 *cdc12 Δ C*-GFP expression is repressed. In these conditions, Gef1-tdTomato localizes to
179 the division site of mitotic cells, which are approximately 14 μ m in length (Fig. 1C).
180 However, induction of *cdc12 Δ C*-GFP expression results in the formation of ectopic rings
181 in mono-nucleate interphase cells less than 10 μ m long, to which Gef1-tdTomato
182 localizes (Fig. 1C). This indicates that Gef1 localization to the ring is not cell cycle-
183 dependent, but rather that formation of the actomyosin ring is sufficient for Gef1
184 localization.

185 Next, we asked what pathway recruits Gef1 to the division site. The Septation Initiation
186 Network (SIN) is a protein signaling network that coordinates the timing of cytokinesis
187 with chromosome segregation (ROBERTS-GALBRAITH AND GOULD 2008; JOHNSON *et al.*
188 2012; SIMANIS 2015). The SIN pathway recruits and activates proteins involved in ring
189 constriction and the coordinated process of septum formation (JIN *et al.* 2006; ROBERTS-
190 GALBRAITH *et al.* 2010; BOHNERT *et al.* 2013). To determine whether the SIN is required
191 for Gef1 localization to the division site, we examined the localization of Gef1-3YFP in

192 two SIN protein kinase *ts* mutants, *plo1-25* and *sid2-250* (BAHLER *et al.* 1998; JIN *et al.*
193 2006; HACHET AND SIMANIS 2008). In *plo1-25* and *sid2-250*, Gef1-3xYFP localizes
194 normally to the division site at the permissive temperature of 25°C. Surprisingly, Gef1-
195 3YFP still localizes to ring like structures in *plo1-25* and *sid2-250* cells shifted to the
196 restrictive temperature of 35.5°C for 1, 2, or 4 hours (Fig. 1D). We imaged *plo1-25* and
197 *sid2-250* cells expressing Gef1-mNG and the ring marker Rlc1-tdTomato to better
198 visualize the ring-like Gef1 structures and to determine whether these structures
199 represented components of the actomyosin ring. Indeed, Gef1-mNG colocalizes with
200 Rlc1-tdTomato in cells shifted to 35.5°C for 1, 2, or 4 hours, demonstrating that Gef1
201 recruitment to the actomyosin ring is not dependent upon the SIN pathway (Fig. 1E).
202 Since we had observed Gef1 localization to cortical nodes, we examined whether Gef1
203 recruitment was Mid1-dependent. Mid1 is an anillin-like protein that is exported from the
204 nucleus to form cortical nodes that define the division plane (BAHLER *et al.* 1998;
205 PAOLETTI AND CHANG 2000). It is to these nodes that various contractile ring components
206 are recruited, before coalescing to form the actomyosin ring (COFFMAN *et al.* 2009;
207 LAPORTE *et al.* 2011). In *mid1Δ* cells, Gef1-3xYFP localizes to misplaced, extended ring-
208 like structures (Fig.1D). Gef1-mNG and Rlc1-tdTomato colocalize at these extended
209 ring-like structures, similarly to the *sin* mutants (Fig.1E). This demonstrates that the
210 early node protein Mid1 is not required for the localization of Gef1 to the actomyosin
211 ring.

212 Closer examination of the division site prior to ring constriction shows patch like Gef1-
213 mNG distribution rather than a continuous ring (Fig. 1A and E). This is in agreement
214 with our observation that Gef1 associates with cytokinetic nodes at the division site
215 upon LatA treatment.

216

217

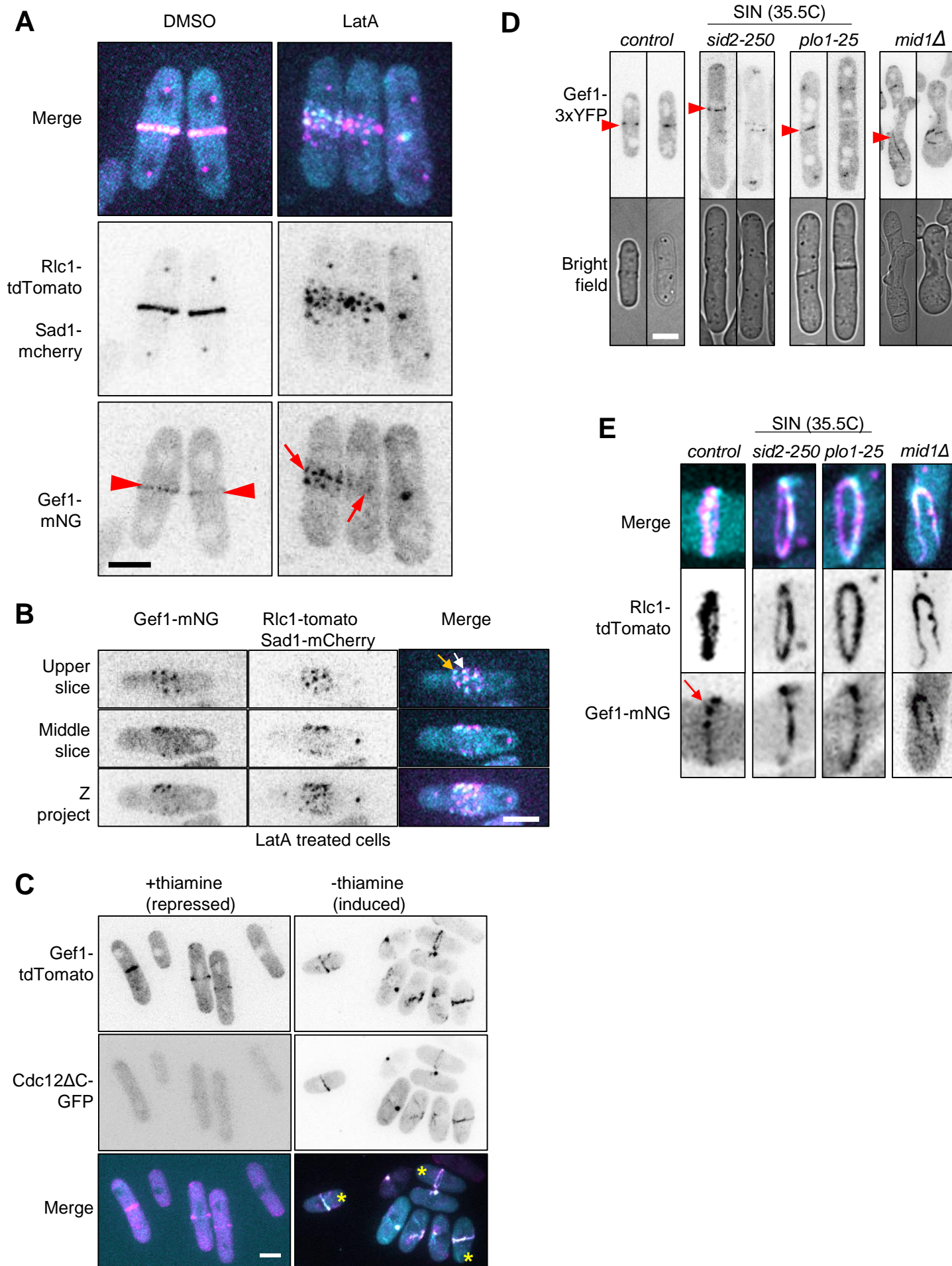


Figure 1

Figure 1. Gef1 associates with cytokinetic nodes. (A) Gef1-mNG and Rlc1-tdTomato localization was examined in cells treated with 10 μ M LatA for 30 min. In DMSO treated control cells, Gef1 (red arrowheads) localizes normally to the actomyosin ring. Upon treatment with the actin depolymerizing drug LatA, the ring fragments and Gef1 appears to localize to cortical nodes at division site (red arrows). **(B)** Top and middle z-series show node like organization of Gef1-mNG and Rlc1-tdTomato about the cortex at the division site in cells treated with LatA. White arrow shows colocalized Gef1 and Rlc1, while orange arrow shows Gef1 alone. **(C)** Expression of *cdc12 Δ C-GFP* induces ectopic actomyosin ring formation and constriction in interphase cells. Gef1-tdTomato ectopically localizes to these rings that form in interphase (yellow asterisks). **(D)** Gef1 localizes to aberrant ring-like structures formed in *sin* and *mid1 Δ* mutants. Indicated genotypes were shifted to the restrictive temperature of 35.5°C for 4 hours. Top row: Inverted max projections of Gef1-3xYFP (red arrowheads). Bottom row: Brightfield images of the representative images above. **(E)** Gef1 colocalizes with Rlc1-tdTomato in the aberrant rings formed in *sin* and *mid1 Δ* mutants. Red arrow shows node like organization of Gef1 at the actomyosin ring in *sid2⁺ plo1⁺ mid1⁺* control cells. Merge of the division site of *control* and *sin* and *mid1 Δ* mutant cells expressing Gef1-mNG and Rlc1-tdTomato. Scale bars represent 5 μ m.

218 **Gef1-dependent Cdc42 activation appears at the division site prior to ring**
219 **assembly**

220 The observation that Gef1 appears to localize to node like patches at the division site
221 upon LatA treatment suggests that Gef1 may also be present in nodes during ring
222 assembly. However, Gef1 is localized mainly in the cytoplasm and cannot be easily
223 detected when present in small quantities at the membrane. Gef1 is the first GEF to
224 localize to the division site and activate Cdc42 (WEI *et al.* 2016). To determine if Gef1
225 indeed localizes to the division site prior to ring assembly, we carefully examined Gef1-
226 mediated Cdc42 activity during ring assembly. We monitored Cdc42 activity with the
227 CRIB-3xGFP bio-probe that specifically binds to active GTP-bound Cdc42 (TATEBE *et al.*
228 2008). In *gef1*⁺ cells, CRIB-3xGFP first appears as a broad band at the division site, as
229 it is lost from the nucleus, 8 minutes after the Sad1-mCherry labelled spindle pole
230 bodies (SPB) separates (Fig. 2A, red arrowhead, 2D). However, the actomyosin ring,
231 visualized by Rlc1-tdTomato, does not fully assemble for another 4 minutes (Fig.2A,
232 blue arrowhead). This suggests that Cdc42 is activated at the cortical nodes before they
233 completely condense to form the cytokinetic ring. In contrast, CRIB-3xGFP does not
234 become active at the division site until ~44 minutes after SPB separation (Fig. 2B, red
235 arrowhead, 2D). Thus, although Gef1 cannot be directly detected at the division site
236 during this period, our findings suggest that Gef1 specifically activates Cdc42 as the
237 ring assembles (Fig. 2B).

238 While our data suggests that Gef1 associates with cortical nodes, its localization is
239 independent of the early node protein, Mid1. Since Gef1-mediated Cdc42 activation
240 initiates during ring formation, we posit that a later node protein may recruit Gef1 to the
241 division site. One of the last proteins recruited to the cortical nodes before ring formation
242 is the F-BAR Cdc15 (WU *et al.* 2003). During cytokinesis Cdc15 is redistributed from the
243 cell tips to the division site. We find that while Cdc15 localizes to the division site ~ 4
244 minutes after SPB separation, patches of Cdc15 remain at the polarized growth regions
245 until ~10 minutes after SPB separation (Fig. 2C, 2D). This suggests that Cdc42 is
246 activated at the division site as Cdc15 is redistributed within the cell. Since Cdc42
247 activation is solely Gef1-mediated during this period, we asked whether Cdc15 may
248 recruit Gef1 to the division site to activate Cdc42. A recent report indicates that Gef1
249 regulates Cdc15 distribution along the actomyosin ring (ONWUBIKO *et al.* 2019). It is
250 possible that Gef1 via a feedback mechanism depends on Cdc15 for its localization.

251

252

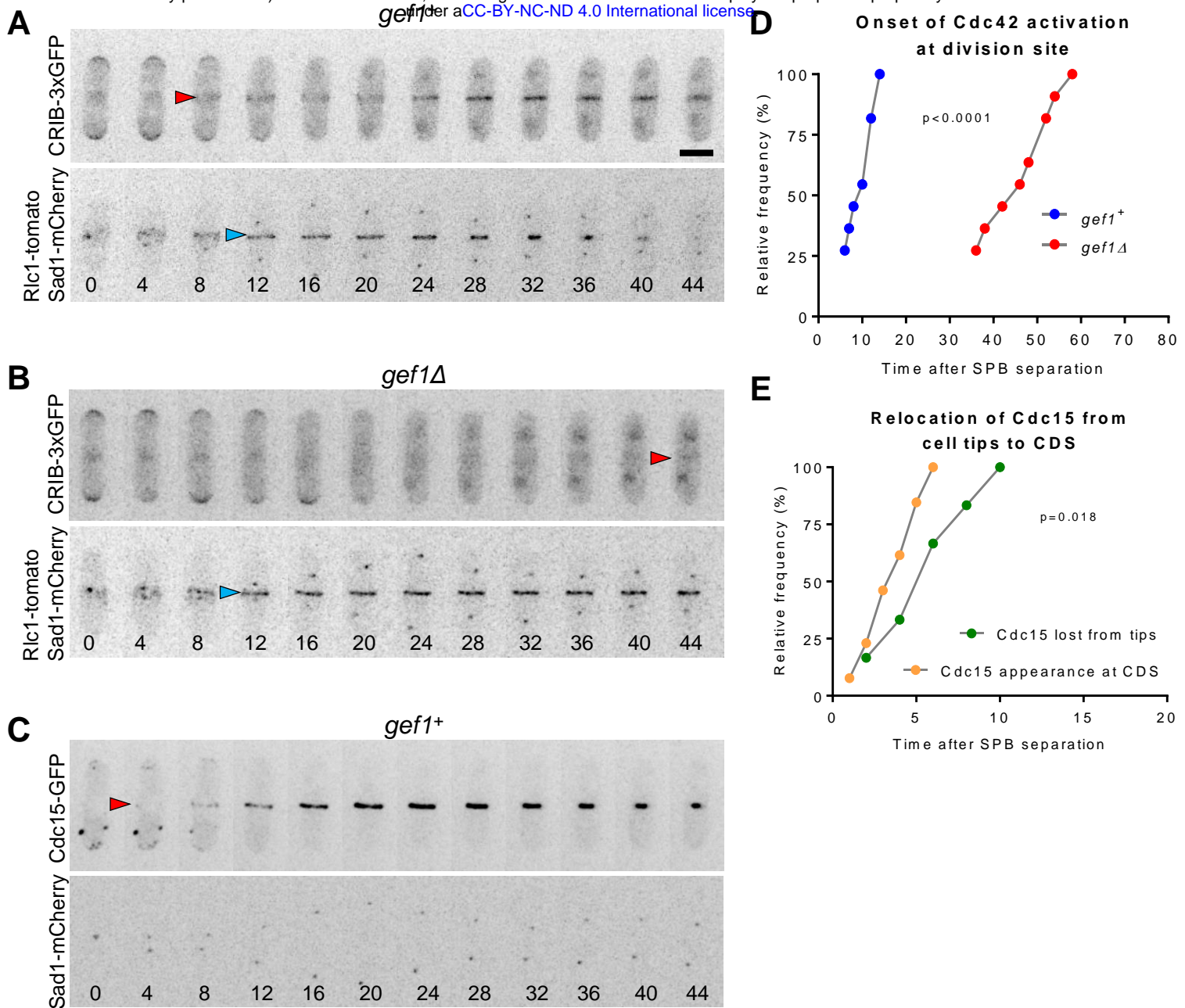


Figure 2

Figure 2. Cdc42 activation at the division site initiates during actomyosin ring formation. (A) In *gef1⁺* cells, CRIB-3xGFP appears at the division site prior to ring assembly. **(B)** In *gef1Δ* cells, CRIB-3xGFP does not appear at the division site until the onset of ring constriction. **(C)** Cdc15-GFP appears at the division site and begins to condense into the ring just prior to Cdc42 activation. Montages are inverted z-projections of the same cells imaged over time. Numbers beneath montages represent time in minutes with respect to SPB separation. Red arrowheads mark the time at which CRIB-3xGFP is first detected at the division site (A and B) or Cdc15-GFP (C). Blue arrowheads mark ring formation. **(D)** Frequency distribution plot of the percentage of cells in the indicated strains with CRIB-3xGFP at the division site as a function of time since SPB separation. **(E)** Frequency distribution plot of the relocation of Cdc15 from the tips to the division site as a function of time since SPB separation. Reported p-values from Student's t-test. Scale bar represents 5 μ m.

253 **Cdc15 promotes Gef1 localization to the division site**

254 Cdc15 associates with the membrane via its F-BAR domain and acts as a scaffold that
255 associates with proteins at the actomyosin ring (MCDONALD *et al.* 2015; REN *et al.* 2015;
256 MCDONALD *et al.* 2017). The scaffolding ability of Cdc15 is primarily conferred through
257 its C-terminal SH3 domain, through which it interacts with other proteins (ROBERTS-
258 GALBRAITH *et al.* 2009; REN *et al.* 2015). While *cdc15* is essential for fission yeast, a
259 *cdc15ΔSH3* mutant is viable but displays defects in septum ingression and ring
260 constriction (ROBERTS-GALBRAITH *et al.* 2009). Similar to *gef1Δ* mutants, onset of ring
261 constriction and Bgs1 localization to the division site is delayed in *cdc15ΔSH3* mutants
262 (ROBERTS-GALBRAITH *et al.* 2009; ARASADA AND POLLARD 2014; CORTES *et al.* 2015; WEI
263 *et al.* 2016). In these mutants the Cdc15 interacting proteins are partially lost from the
264 division site (REN *et al.* 2015). We posit that Cdc15 may promote Gef1 localization to
265 the division site through interaction with its SH3 domain. To test this, we examined
266 Gef1-tdTomato localization to rings that were assembled, but not constricting, in cells
267 expressing either Cdc15-GFP or *cdc15ΔSH3*-GFP. Gef1-tdTomato is present in ~70%
268 of Cdc15-GFP rings, while Gef1-tdTomato is present in only ~40% of *cdc15ΔSH3*-GFP
269 rings (Fig. 3A and Fig. 3B). Furthermore, Gef1-tdTomato fluorescent intensity is also
270 reduced at the assembled rings of the *cdc15ΔSH3* mutant, with a relative intensity of
271 only 76% that of *cdc15⁺* cells (Fig. 3A, 3C, Table 1). We find that Gef1-tdTomato
272 localizes to the division site in cells with a minimum SPB distance of 3μm in *cdc15⁺*
273 cells. In contrast, in *cdc15ΔSH3* mutants Gef1-tdTomato appears at the division site
274 with a minimum SPB distance of 7μm (Table 1). Moreover, in *cdc15⁺* cells 61% of cells
275 in anaphase B displayed Gef1-tdTomato at the division site, while in *cdc15ΔSH3*
276 mutants only 12% of anaphase B cells showed Gef1 localization (Table 1). While Gef1
277 localization to assembled rings is initially impaired in cells expressing *cdc15ΔSH3*-GFP,
278 all constricting rings have Gef1-tdTomato (Table 1). This suggests that Cdc15 may
279 either initially stabilize Gef1 or promote its localization to the division site.

280

281

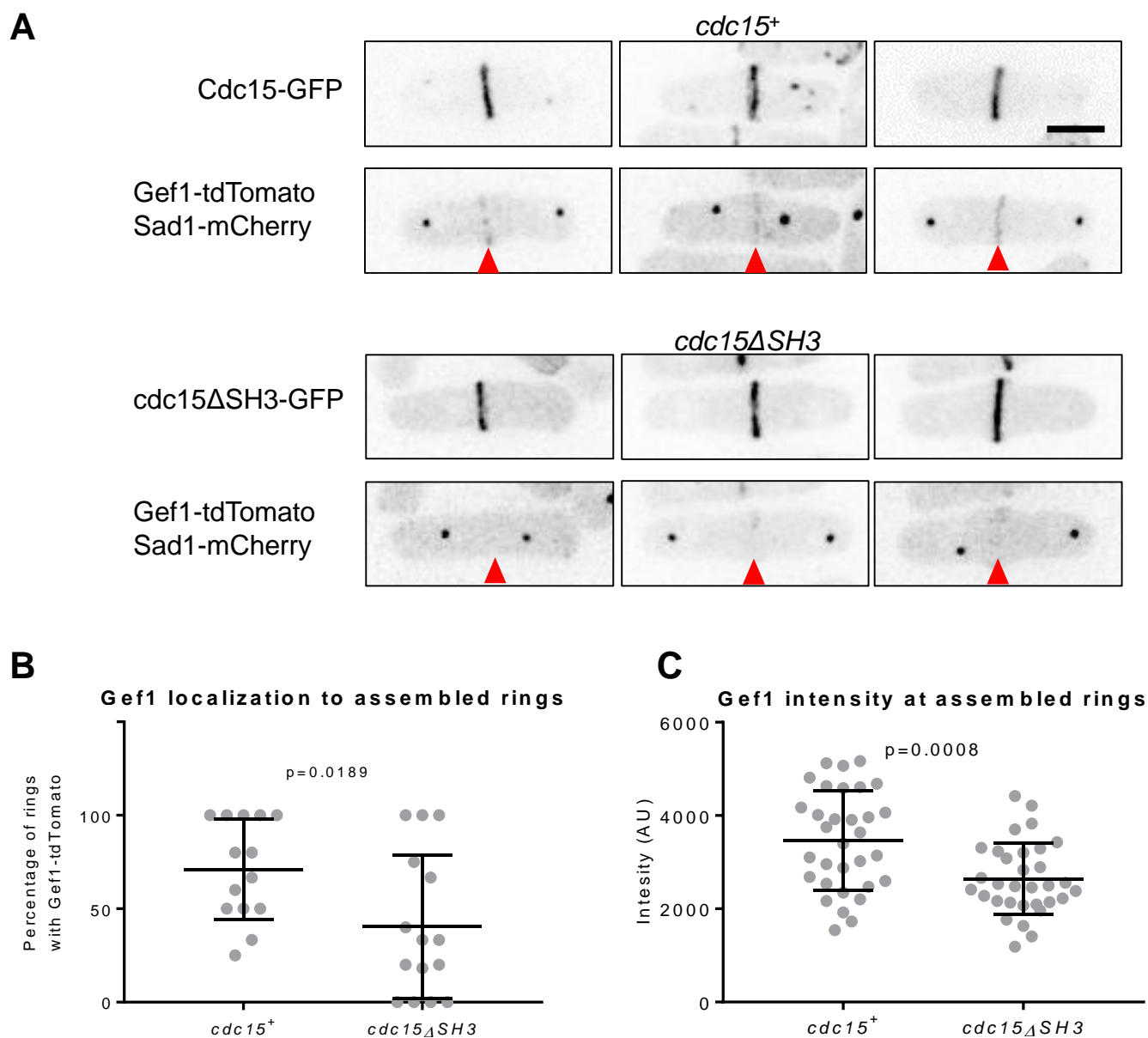


Figure 3

Figure 3. Cdc15 promotes Gef1 localization to the division site. (A) Inverted max projections of *cdc15⁺* and *cdc15 Δ SH3* expressing Cdc15-GFP, Gef1-tdTomato, and Sad1-mCherry. Red arrowheads mark the division site. (B) Quantification of fields of cells of the indicated genotypes that have Gef1-tdTomato present at the assembled actomyosin ring. (C) Quantification of Gef1-tdTomato intensity at assembled, but not constricting, rings in the indicated genotypes. Reported p-values from Student's t-test. Scale bar represents 5 μ m.

Table 1. Characterization of Gef1 recruitment to the division site in a *cdc15*-dependent manner

	SPB distance at which Gef1 first appears at CDS	% of Anaphase B cells with Gef1 at CDS	% of cells with assembled rings with Gef1 at CDS	% of cells with assembled rings with Gef1 at CDS	Relative Gef1-tdTomato intensity
<i>cdc15</i> ⁺	3 μ m N=26	61% N=26	78% N=56	100% N=24	1.0 N=32
<i>cdc15</i> Δ <i>SH3</i>	7 μ m n=26	12% n=26	48% n=37	100% n=43	0.76 n=32

282 ***cdc15* phenocopies *gef1* polarity phenotypes**

283 Our data indicates a functional relationship between Gef1 and Cdc15 during
284 cytokinesis. This is further supported by the fact that *cdc15* Δ *SH3* and *gef1* share a
285 common phenotype: a delay in the onset of ring constriction and Bgs1 localization at the
286 division site (ARASADA AND POLLARD 2014; CORTES *et al.* 2015; WEI *et al.* 2016). It is
287 possible that during cytokinesis Cdc15 recruits Bgs1 to the division site through Gef1.
288 Since *gef1* has been shown to regulate cell polarity, we asked if *cdc15* functionally
289 interacts with Gef1 during cell polarization. *gef1* Δ cells are primarily monopolar,
290 growing only from the old end (COLL *et al.* 2003; DAS *et al.* 2015). In contrast, the
291 hypermorphic allele *gef1S112A* exhibits precocious new end growth, producing
292 primarily bipolar cells (DAS *et al.* 2015). We asked if this functional relationship between
293 Gef1 and Cdc15 is specific to cytokinesis, or whether it is also observed during
294 polarized growth. Indeed, as compared to control cells *cdc15* Δ *SH3* mutants show
295 decreased bipolarity in interphase cells, similar to that observed in *gef1* Δ cells (Fig. 4A,
296 4B). Next, we asked if an increase in bipolarity was also observed in *cdc15* mutants with
297 increased cortical localization. When oligomerized, the F-BAR domain enables Cdc15 to
298 properly interact with the membrane (ROBERTS-GALBRAITH *et al.* 2010; McDONALD *et al.*
299 2015). Cdc15 is a phospho-protein where hyper-phosphorylation disrupts proper
300 oligomerization and at least in part impairs function (ROBERTS-GALBRAITH *et al.* 2010). In
301 contrast, the de-phosphorylated form of Cdc15 shows increased oligomerization and
302 increased localization at cortical patches (ROBERTS-GALBRAITH *et al.* 2010). We find that
303 similar to *gef1* Δ and *cdc15* Δ *SH3* mutants, the phosphomimetic *cdc15-27D* allele
304 exhibits decreased bipolarity (Fig. 4A, 4B). Further, the non-phosphorylatable *cdc15-27A*
305 allele is primarily bipolar, similar to *gef1S112A* mutants (Fig. 4A, 4B). These results
306 demonstrate that, as during cytokinesis, *cdc15* functionally interacts with *gef1* also
307 during cell polarization.

308

309

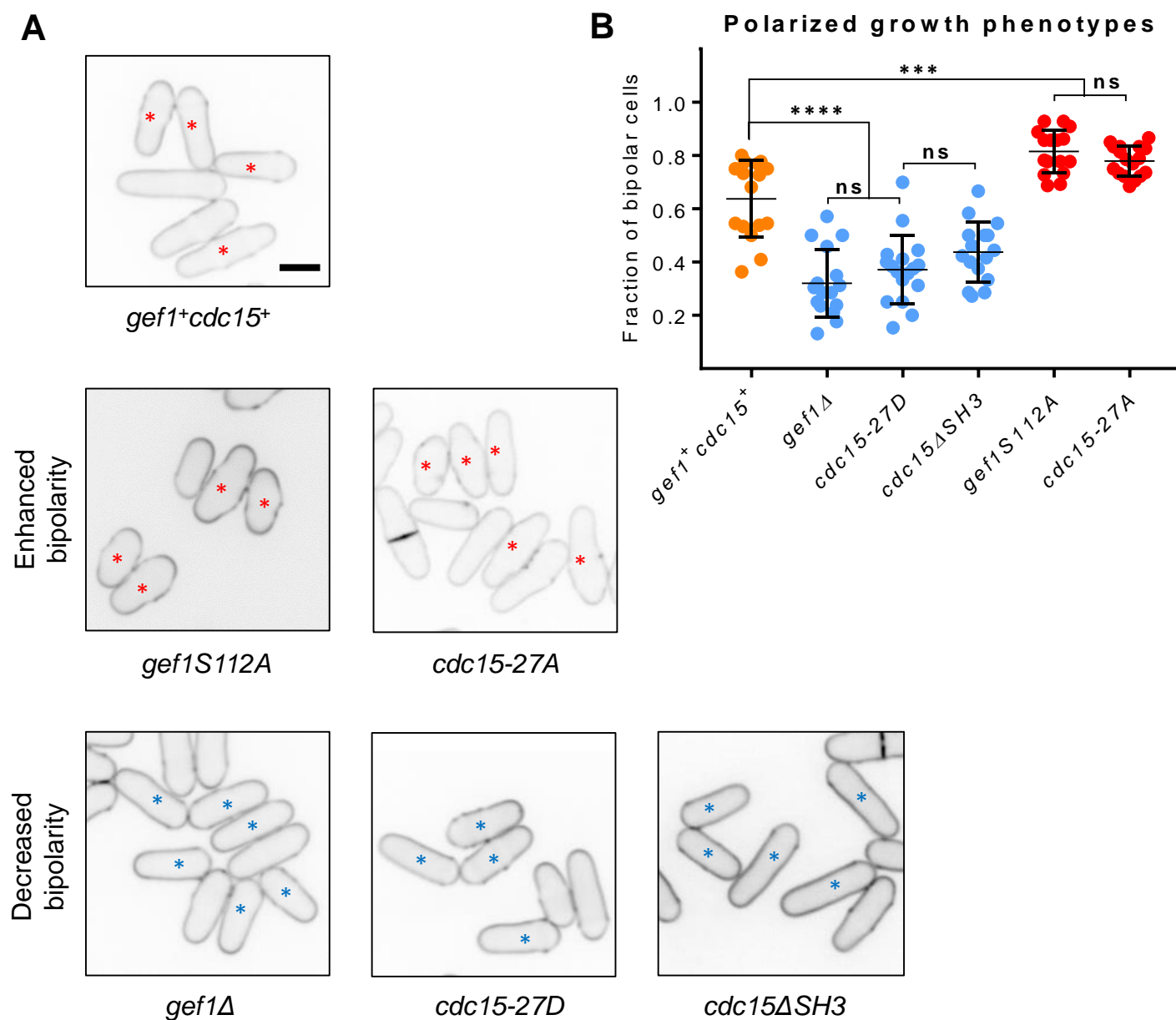


Figure 4

Figure 4. *cdc15* phenocopies *gef1* polarity phenotypes. (A) Representative images of the indicated genotypes stained with calcofluor to visualize polarized growth. Red asterisks denote bipolar cells, blue asterisks mark monopolar cells. (B) Quantification of the polarized growth phenotypes in the indicated genotypes. (****, $p < 0.0001$, ***, $p < 0.001$, ns, not significant, p-values reported from ANOVA with Tukey's multiple comparisons post hoc test). Scale bar represents 5 μ m.

310 ***cdc15-27A* enhances Gef1 localization at cortical patches and division site**

311 Gef1 is predominantly a cytosolic GEF, at least during interphase, and only transiently
312 localizes to sites of polarized growth (DAS *et al.* 2015). Given that Cdc15 promotes the
313 recruitment of Gef1 to the division site, we asked whether it may also promote its
314 localization to the sites of polarized growth, as suggested by the polarity phenotypes
315 exhibited by *cdc15* mutants. While Cdc15-GFP is clearly visible at endocytic patches at
316 the cell tips, Gef1-tdTomato is seldom observed (Fig. 5A, i). The non-phosphorylatable
317 *cdc15-27A* mutants tagged to GFP show increased localization at cortical patches
318 during interphase. Correspondingly, in cells expressing *cdc15-27A*-GFP, Gef1-
319 tdTomato is readily observed at the cell cortex (Fig. 5A, ii, iii). Moreover, we also
320 observed colocalization of Gef1-tdTomato and *cdc15-27A*-GFP at the cortical patches
321 (Fig. 5A, v, red arrow). Interestingly, in addition to these colocalized patches, some
322 regions of the cortex contain only Gef1-tdTomato or Cdc15-GFP (Fig. 5A, iv, green and
323 orange arrowheads respectively). Next, we asked if Cdc15 also promoted Gef1
324 localization to the division site. We observe Gef1-mediated Cdc42 activation at the
325 division site well before Gef1 itself is detectable (Fig. 1A). Similar to a previous report,
326 Gef1-tdTomato can be detected at the division site only in rings that have completed
327 assembly (WEI *et al.* 2016). We find that in *cdc15-27A* mutants, Gef1-tdTomato
328 localizes to the division site before the ring completes assembly. Gef1-tdTomato
329 colocalizes with *cdc15-27A*-GFP as the latter condenses into a ring, while it is not yet
330 detectable at this stage in *cdc15*⁺ cells (Fig. 5B). Since it is hard to distinguish Gef1
331 signal at the division site from the cytoplasmic signal, it is not possible to precisely
332 determine when Gef1 localizes to the division site by time lapse microscopy. However,
333 we find that Gef1-tdTomato is detectable at cortical nodes in the medial region of
334 interphase cells (Fig. 5C, yellow circles). Thus, it is possible that Gef1 localizes earlier
335 to the division site in *cdc15-27A* mutants.

336 Next, we addressed whether Cdc15 specifically interacts with Gef1 or whether this
337 interaction also extends to the other Cdc42 GEF. We examined the localization of the
338 Cdc42 GEF Scd1 in *cdc15-27A* mutants. Under normal conditions, Scd1-tdTomato
339 localization appears as a cap at the cell tips during interphase (KELLY AND NURSE 2011;
340 DAS *et al.* 2012). We find that Scd1-tdTomato localization in *cdc15-27A* cells does not
341 differ from *cdc15*⁺ cells and do not localize to interphase cortical patches and nodes
342 (Fig. 5D). This indicates that Cdc15 specifically promotes Gef1 localization during
343 cytokinesis and cell polarization.

344

345

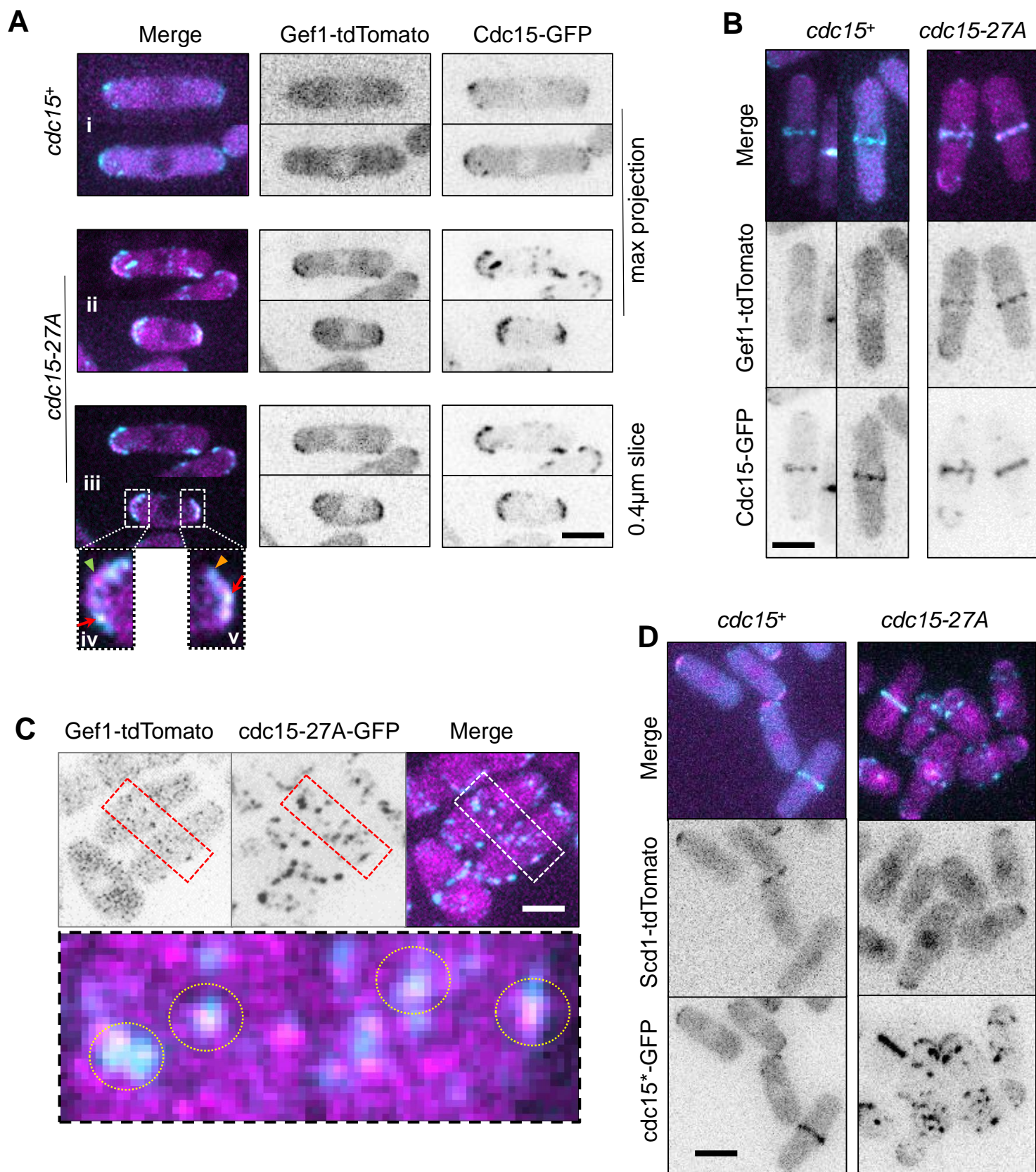


Figure 5

Figure 5. *cdc15-27A* enhances Gef1 localization at cortical patches. (A) Gef1-tdTomato and Cdc15-GFP localization to cortical patches in interphase *cdc15*⁺ and *cdc15-27A* cells. **i** and **ii** are max projections, while **iii** is a single 0.4 μ m z-plane of the same cell in **ii**. Insets **iv** and **v** are enlarged regions of the cell poles marked by white boxes. Red arrows indicate colocalization of Gef1 and Cdc15 patch. Green arrowhead indicates a Gef1 patch that does not colocalize with Cdc15. Orange arrowhead indicates a Cdc15 patch that does not colocalize with Gef1. **(B)** Gef1-tdTomato and Cdc15-GFP localization to the division site in *cdc15*⁺ and *cdc15-27A* cells. **(C)** Gef1-tdTomato and Cdc15-GFP localization to cortical patches at the division site in interphase *cdc15*⁺ and *cdc15-27A* cells. Yellow circles indicate colocalization of Gef1 and Cdc15 patch. Inset is an enlarged region of nascent division site marked by white box. **(D)** Scd1-tdTomato localization in *cdc15*-GFP and *cdc15-27A*-GFP expressing cells. Scale bar represents 5 μ m.

346 **Cdc15 promotes Gef1-mediated Cdc42 activation**

347 Given that Gef1 precociously localizes to nodes at the division site of cells expressing
348 *cdc15-27A*, we asked whether this was concomitant with precocious Cdc42 activation.
349 Normally Cdc42 activity, visualized by CRIB-3xGFP, first appears at the division site
350 only after the cell initiates anaphase A (WEI *et al.* 2016). However, we find that in *cdc15-*
351 *27A* mutants, CRIB-3xGFP signal was visible at the cell medial region, even before the
352 Sad1-mCherry labelled SPB separated. In these cells CRIB-3xGFP signal appeared as
353 a broad band that overlapped with the nucleus (Fig. 6A). Next, we performed time lapse
354 microscopy to determine when Cdc42 was activated at the division site in *cdc15-27A*
355 mutants. Cdc42 is first activated ~10 minutes after SPB separation in *cdc15+* cells. We
356 find that in *cdc15-27A* mutants, Cdc42 is activated earlier at ~4 minutes after SPB
357 separation, as determined by CRIB-3xGFP localization (Fig. 6B, red arrowhead,
358 Supplementary Fig. S1). Further, similar to previous reports, in *cdc15+* cells CRIB-
359 3xGFP signal at the division site appears concurrent to loss of signal from the cell tips.
360 We find that in *cdc15-27A* mutants, CRIB-3xGFP signal at the division site appears well
361 before the signal is lost from the cell tips (Fig. 6B, yellow asterisk). While CRIB-3xGFP
362 signal at the cell medial region is clearly detected in cells with a single SPB by still
363 imaging, we did not detect CRIB-3xGFP signal at the division site prior to SPB
364 separation by time lapse imaging. This could be due to low abundance or
365 photobleaching of the signal, or it is possible that Cdc42 is only transiently activated at
366 the medial region during interphase in *cdc15-27A* cells.

367 Finally, we asked if the premature CRIB-3xGFP signal at the division site and the
368 increased bipolarity observed in *cdc15-27A* mutants was due to Gef1-mediated Cdc42
369 activation. To test this, we deleted *gef1* in *cdc15-27A* mutants. While *cdc15-27A*
370 mutants display an increased number of bipolar cells, the number of bipolar cells in the
371 *gef1Δ cdc15-27A* double mutant was significantly reduced ($p < 0.0001$) and similar to that
372 observed in *gef1Δ* mutants (Fig. 7A, 7C). Furthermore, *cdc15-27A* cells display an
373 increase in bipolar CRIB-3xGFP localization at the cell tips, relative to *cdc15+* cells (Fig.
374 7B, 7D, $p = 0.039$). This is consistent with our calcofluor data, indicating that bipolar
375 growth is enhanced by *cdc15-27A*. Deletion of *gef1* in *cdc15-27A* mutants reduces
376 bipolar CRIB-3xGFP localization, similar to that observed in *gef1Δ* cells (Fig. 7B, D,
377 $p < 0.0001$). Likewise, premature Cdc42 activation at the division site in *cdc15-27A*
378 mutants is also abrogated in *gef1Δ cdc15-27A* cells. In *gef1Δ cdc15-27A* mutants CRIB-
379 3xGFP did not appear at the division site until ~45 minutes after SPB separation, as was
380 also observed in *gef1Δ* (Fig. 7E; Supplementary Fig. S1). Together, these results
381 indicate that Cdc15 promotes Cdc42 activation during cytokinesis and cell polarization
382 via Gef1 localization.

383

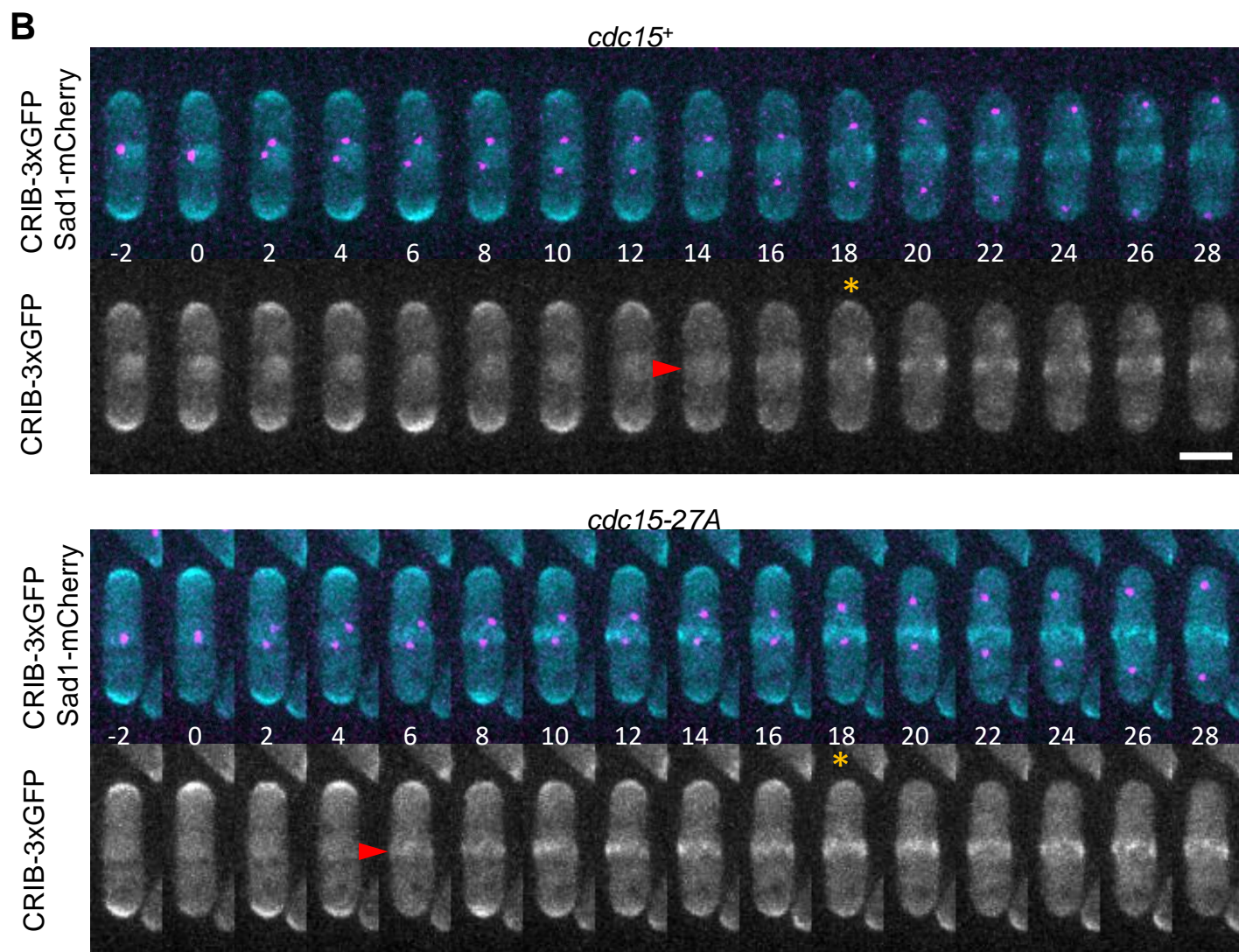
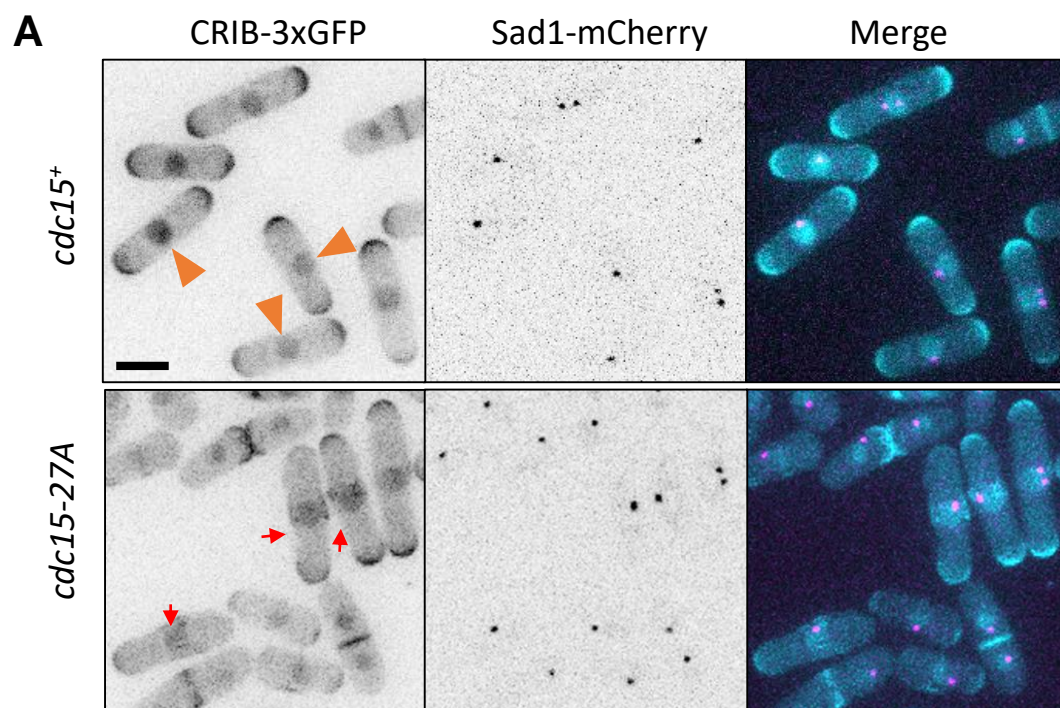


Figure 6

Figure 6. Cdc42 is prematurely activated in *cdc15-27A* cells during cytokinesis. (A) Inverted max projections of the indicated genotypes expressing CRIB-3xGFP and Sad1-mCherry. Orange arrowheads mark interphase cells without CRIB-3xGFP at the division site. Red arrows mark interphase cells with premature Cdc42 activation at the division site. **(B)** Time lapse montages of *cdc15+* and *cdc15-27A* cells expressing CRIB-3xGFP and Sad1-mCherry. Red arrowheads mark onset of Cdc42 activation at the division site. Orange asterisks mark last time points before Cdc42 is completely lost from the cell tips. Numbers beneath montages represent time in minutes with respect to SPB separation. Scale bar represents 5 μ m.

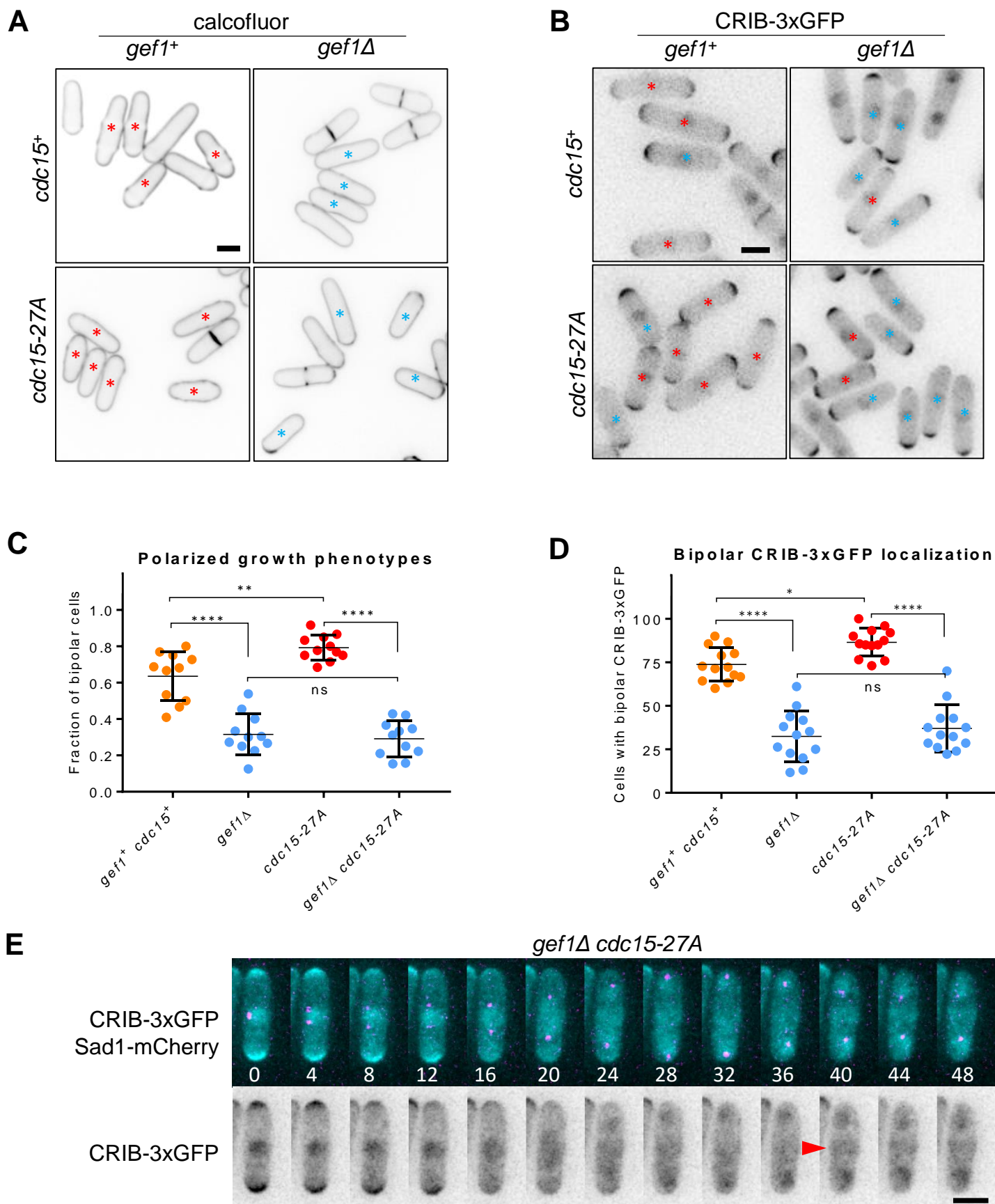


Figure 7

Figure 7. Cdc15 promotes Gef1-mediated Cdc42 activation. (A) Representative images of the indicated genotypes stained with calcofluor to visualize polarized growth. Red and blue asterisks denote bipolar and monopolar cells, respectively. **(B)** Quantification of the polarized growth phenotypes in the indicated genotypes. **(C)** Inverted max projections of the indicated strains expressing CRIB-3xGFP. Red asterisks mark cells with bipolar CRIB, blue asterisks show cells with monopolar CRIB localization. **(D)** Quantification of CRIB-3xGFP localization in the indicated genotypes. **(E)** Time lapse montages of *gef1Δ cdc15-27A* cells expressing CRIB-3xGFP and Sad1-mCherry. Red arrowheads mark onset of Cdc42 activation at the division site. Numbers beneath montages represent time in minutes with respect to SPB separation. (****, $p < 0.0001$, ***, $p < 0.001$, ns, not significant, one-way ANOVA with Tukey's multiple comparisons post hoc test). Scale bar represents 5 μm .

384 DISCUSSION

385 The two Cdc42 GEFs, while partially redundant, show distinct phenotypes during cell
386 polarity and cytokinesis (CHANG *et al.* 1994; COLL *et al.* 2003; WEI *et al.* 2016). This
387 suggests that the GEFs may be regulated in different ways to precisely activate Cdc42
388 at its site of function. Although the role of the Cdc42 GEF, Gef1 in cytokinesis and cell
389 polarity is well established (DAS AND VERDE 2013; CHIOU *et al.* 2017), it is not clear how
390 Gef1 localizes to its site of action. Here we show that Gef1, but not the other GEF Scd1,
391 localizes to its site of action in a manner dependent on the F-BAR Cdc15.

392 Disintegration of the actomyosin ring by LatA treatment results in Gef1 localizing to the
393 cytokinetic nodes suggesting that Gef1 associates with these structures. Gef1 does not
394 become visible at the division site until the nodes coalesce into the actomyosin ring (WEI
395 *et al.* 2016). However, Gef1-dependent Cdc42 activity can be observed a few minutes
396 before the nodes fully coalesce to form the ring. Given that Gef1 is a low abundance
397 protein, it is possible that Gef1 may be present at quantities beneath our detection limit
398 at the cortical nodes during the initial stages of ring assembly.

399 Given the timing of Cdc42 activation, Gef1 appears to be recruited late during the ring
400 assembly process. Thus, we looked at other proteins that are likewise recruited to the
401 cytokinetic nodes during a similar time frame. It has previously been reported that the F-
402 BAR protein Cdc15 is one of the last proteins to be recruited to the cytokinetic nodes
403 before the ring assembles (WU *et al.* 2003). We find that Cdc15 localizes to the division
404 site shortly before Gef1-dependent Cdc42 activity initiates. This seemed a likely
405 candidate for Gef1 recruitment, as Cdc15 serves as a scaffold for many other proteins
406 during cytokinesis. The Cdc15 scaffolding activity is dependent on its C-terminal SH3
407 domain (REN *et al.* 2015). We asked whether Cdc15 recruited Gef1 to the division site
408 via the SH3 domain. We find that Gef1 recruitment is delayed in *cdc15ΔSH3* cells, and
409 Gef1 levels at the division site remain low throughout constriction. Thus, our data
410 suggests that Gef1 localization to the division site is *cdc15* dependent. The F-BAR Imp2
411 also stabilizes proteins at the actomyosin ring via its SH3 domain. While loss of one of
412 these SH3 domains is permissible, the actomyosin ring of *imp2ΔSH3 cdc15ΔSH3*
413 double mutant does not retain its cohesion and disintegrates without constriction
414 (ROBERTS-GALBRAITH *et al.* 2009; REN *et al.* 2015). It is possible that like Cdc15, Imp2
415 may also recruit or stabilize Gef1 at the division site.

416 We have previously reported that the β-1,3-glucan synthase Bgs1, the septum
417 synthesizing enzyme that drives membrane ingression, is delayed in *gef1Δ* cells (WEI *et al.*
418 *et al.* 2016). A similar defect is observed in *cdc15ΔSH3* (ROBERTS-GALBRAITH *et al.* 2009;
419 CORTES *et al.* 2015). Given that Cdc15 promotes Gef1 localization to the division site,
420 and that *cdc15ΔSH3* also exhibits the delayed onset of ring constriction (ROBERTS-
421 GALBRAITH *et al.* 2009), characteristic of *gef1Δ* cells, we posited that Cdc15 acts

422 upstream of Gef1 during cytokinesis. Apart from its role in cytokinesis, Gef1 is also
423 required for proper cell polarity establishment (COLL *et al.* 2003). In fission yeast,
424 immediately after division the cells grow in a monopolar manner from the old end and;
425 as the cells reach a certain size, bipolarity ensues (DAS *et al.* 2012; DAS *et al.* 2015).
426 Loss of *gef1* leads to a delay in initiation of bipolarity and as a result a large number of
427 the cells in interphase are monopolar (COLL *et al.* 2003; DAS *et al.* 2015). We asked if
428 the relationship between Gef1 and Cdc15 was also conserved during cell polarity
429 establishment. Thus, we examined the polarity phenotype of various *cdc15* mutants.
430 Cdc15 is regulated via phosphorylation, and the phospho-mimetic allele *cdc15-27D* has
431 been shown to adopt a closed conformation under cryo-EM, potentially reducing its
432 ability to interact with other proteins (ROBERTS-GALBRAITH *et al.* 2010). Conversely, the
433 non-phosphorylatable allele *cdc15-27A* adopts an open conformation that readily
434 oligomerizes and is potentially hypermorphic (ROBERTS-GALBRAITH *et al.* 2010). While
435 Gef1 mainly localizes to the cytoplasm, its cortical localization is enhanced in *gef1S112A*
436 mutants rendering the cells bipolar. We find that the gain of function *cdc15-27A* mutant
437 resembles *gef1S112A* mutants, in which the cells are predominantly bipolar. In contrast,
438 *cdc15-27D* and *cdc15 Δ SH3* mutants mimic *gef1 Δ* mutants, in which cells are
439 predominantly monopolar. Thus, *cdc15* phenocopies *gef1* during cytokinesis as well as
440 in polarity establishment, providing further evidence of a functional interaction between
441 these proteins.

442 A recent report suggests that Gef1 is primarily a cytosolic GEF, where it activates
443 Cdc42 (TAY *et al.* 2018). Rather our data suggest that Cdc15 recruits Gef1 to the
444 cortical patches to promote bipolar growth. During interphase Cdc15 is localized to the
445 endocytic patches where it promotes vesicle internalization (ARASADA AND POLLARD
446 2011). In the hypermorphic mutants, *cdc15-27A*-GFP levels are elevated at cortical
447 patches (ROBERTS-GALBRAITH *et al.* 2010). Correspondingly, these mutants also show
448 Gef1 localization to these patches. Moreover, Gef1 localization at the cortex is quite
449 prominent in these mutants. In agreement with increased Gef1 cortical localization, we
450 also observe increased Cdc42 activation at both the cell poles resulting in increased
451 bipolarity. A recent paper demonstrates that Gef1 regulates Cdc15 by controlling the
452 size and lifetime of Cdc15 cortical patches (ONWUBIKO *et al.* 2019). Above, we present
453 data that demonstrate Cdc15 is upstream of Gef1. These two observations are not
454 contradictory, but rather reveal an elegant regulatory pattern: Cdc15 recruits Gef1 to
455 endocytic patches, where Gef1 in turn regulates the size of the Cdc15 patch via Cdc42
456 activation. Our observation that Gef1-tdTomato and Cdc15-27A-GFP do not perfectly
457 colocalize at the cortex can be explained by the following model. Cdc15 initially recruits
458 Gef1 to endocytic patches at the cortex, resulting in colocalization. Once Gef1 facilitates
459 patch internalization, Cdc15 is lost from the cortex while Gef1 still persists. Further
460 investigations will determine how Gef1 mediated Cdc42 activity regulates Cdc15 cortical
461 patch lifetime. Given the abundance of Gef1 in the cytoplasm, small levels of Gef1 are

462 not easily detectable at cortical patches. Gef1 localization to the cortical patches and
463 the cortex may be enhanced by the increased abundance of *cdc15-27A* at cortical
464 patches.

465 Since we established that *cdc15* promotes Gef1 localization to the division site, and that
466 *cdc15-27A* enhances Gef1 localization to cell tips, we asked whether *cdc15-27A* would
467 similarly result in precocious Gef1 localization to the division site. Indeed, we find that
468 Gef1 localizes to node like patches at the cell equator in interphase cells. In keeping
469 with this observation, Gef1 was detected during early stages of *cdc15-27A*-labelled ring
470 assembly, while it is not yet detectable at the comparable time in *cdc15⁺* cells. Further,
471 we show that precocious Gef1 localization results in premature Cdc42 activation.
472 Finally, we show that the *cdc15* mutant phenotypes, which arise from the mis-regulation
473 of Cdc42, are *gef1*-dependent. While *cdc15-27A* cells are mainly bipolar, loss of *gef1* in
474 these cells reverts to the *gef1* Δ monopolarity phenotype. Cdc42 activation at the
475 division site is also delayed in *cdc15-27A gef1* Δ . Together these results indicate that
476 *gef1* is epistatic to *cdc15*.

477 The mechanistic understanding of factors that control Gef1 localization is sorely lacking.
478 Aside from the observation that the N-terminus of Gef1 is required for its localization to
479 the membrane, no other factors have been identified (DAS *et al.* 2015). It has also been
480 reported that Gef1 activates Cdc42 with the help of N-BAR Hob3 protein interaction
481 (COLL *et al.* 2007). Gef1 is a homolog of the mammalian GEF TUBA and contains an N-
482 BAR domain (DAS *et al.* 2015). However, previous reports show that the Gef1-N-BAR
483 domain is not required for its localization to the division site, nor is Hob3 required for
484 Gef1 localization (Supplementary Fig. S2) (DAS *et al.* 2015). In contrast, the
485 mechanism removing Gef1 from the membrane has been elucidated. Gef1 is
486 phosphorylated by Orb6, generating a 14-3-3 binding site that results in Gef1 removal
487 by Rad24 (DAS *et al.* 2009; DAS *et al.* 2015). Here, we identify Cdc15 as a factor that
488 promotes Gef1 localization to both the cell tips and division site. A recent study
489 indicates that Gef1-mediated Cdc42 activation regulates endocytosis, by controlling the
490 lifetime of Cdc15 on endocytic patches (ONWUBIKO *et al.* 2019). The role of endocytosis
491 in cell polarity is well established and its role in cytokinesis is increasingly recognized
492 (WANG *et al.* 2016; ONWUBIKO *et al.* 2019). Taken together, this suggests that Cdc15
493 promotes Gef1-mediated Cdc42 activation to regulate endocytosis to promote both
494 bipolar growth and cytokinesis. We find that Cdc15 promotes the localization of Gef1,
495 but not Scd1. These studies begin to explain how, through differential regulation and
496 localization, two GEFs of the same GTPase can exhibit distinct phenotypes.

497

498

499

500 **ACKNOWLEDGEMENTS**

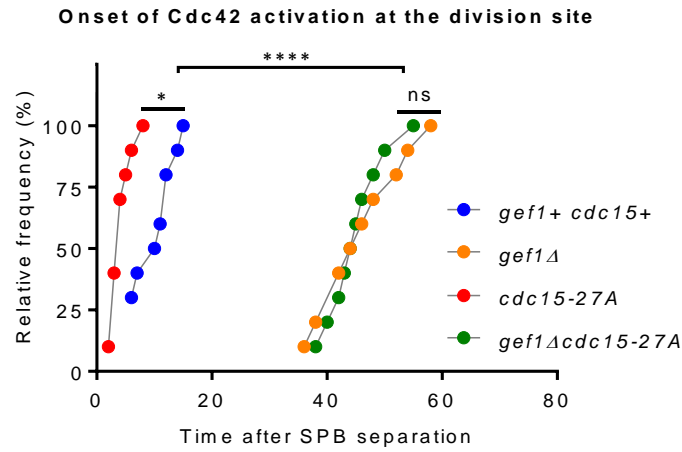
501 We thank Kathleen Gould and Fred Chang for generously providing strains. This work
502 was funded by National Science Foundation, grant #1616495.

503 REFERENCES

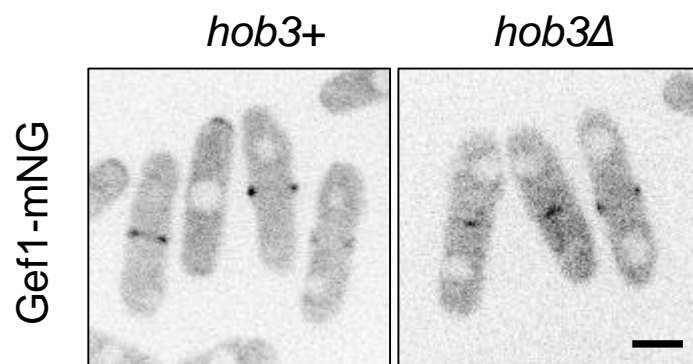
- 504 Arasada, R., and T. D. Pollard, 2011 Distinct roles for F-BAR proteins Cdc15p and Bzz1p in actin
505 polymerization at sites of endocytosis in fission yeast. *Curr Biol* 21: 1450-1459.
- 506 Arasada, R., and T. D. Pollard, 2014 Contractile ring stability in *S. pombe* depends on F-BAR protein
507 Cdc15p and Bgs1p transport from the Golgi complex. *Cell Rep* 8: 1533-1544.
- 508 Bahler, J., A. B. Steever, S. Wheatley, Y. Wang, J. R. Pringle *et al.*, 1998 Role of polo kinase and Mid1p in
509 determining the site of cell division in fission yeast. *J Cell Biol* 143: 1603-1616.
- 510 Bohnert, K. A., A. P. Grzegorzewska, A. H. Willet, C. W. Vander Kooi, D. R. Kovar *et al.*, 2013 SIN-
511 dependent phosphoinhibition of formin multimerization controls fission yeast cytokinesis.
512 *Genes Dev* 27: 2164-2177.
- 513 Bos, J. L., H. Rehmann and A. Wittinghofer, 2007 GEFs and GAPs: critical elements in the control of small
514 G proteins. *Cell* 129: 865-877.
- 515 Chang, E. C., M. Barr, Y. Wang, V. Jung, H. P. Xu *et al.*, 1994 Cooperative interaction of *S. pombe* proteins
516 required for mating and morphogenesis. *Cell* 79: 131-141.
- 517 Chiou, J. G., M. K. Balasubramanian and D. J. Lew, 2017 Cell Polarity in Yeast. *Annu Rev Cell Dev Biol* 33:
518 77-101.
- 519 Coffman, V. C., A. H. Nile, I. J. Lee, H. Liu and J. Q. Wu, 2009 Roles of formin nodes and myosin motor
520 activity in Mid1p-dependent contractile-ring assembly during fission yeast cytokinesis. *Mol Biol*
521 *Cell* 20: 5195-5210.
- 522 Coll, P. M., S. A. Rincon, R. A. Izquierdo and P. Perez, 2007 Hob3p, the fission yeast ortholog of human
523 BIN3, localizes Cdc42p to the division site and regulates cytokinesis. *The EMBO journal* 26: 1865-
524 1877.
- 525 Coll, P. M., Y. Trillo, A. Ametzazurra and P. Perez, 2003 Gef1p, a new guanine nucleotide exchange factor
526 for Cdc42p, regulates polarity in *Schizosaccharomyces pombe*. *Molecular biology of the cell* 14:
527 313-323.
- 528 Cortes, J. C., N. Pujol, M. Sato, M. Pinar, M. Ramos *et al.*, 2015 Cooperation between Paxillin-like Protein
529 Pxl1 and Glucan Synthase Bgs1 Is Essential for Actomyosin Ring Stability and Septum Formation
530 in Fission Yeast. *PLoS Genet* 11: e1005358.
- 531 Das, M., T. Drake, D. J. Wiley, P. Buchwald, D. Vavylonis *et al.*, 2012 Oscillatory Dynamics of Cdc42
532 GTPase in the Control of Polarized Growth. *Science*.
- 533 Das, M., I. Nunez, M. Rodriguez, D. J. Wiley, J. Rodriguez *et al.*, 2015 Phosphorylation-dependent
534 inhibition of Cdc42 GEF Gef1 by 14-3-3 protein Rad24 spatially regulates Cdc42 GTPase activity
535 and oscillatory dynamics during cell morphogenesis. *Mol Biol Cell*.
- 536 Das, M., and F. Verde, 2013 Role of Cdc42 dynamics in the control of fission yeast cell polarization.
537 *Biochem Soc Trans* 41: 1745-1749.
- 538 Das, M., D. J. Wiley, X. Chen, K. Shah and F. Verde, 2009 The conserved NDR kinase Orb6 controls
539 polarized cell growth by spatial regulation of the small GTPase Cdc42. *Curr Biol* 19: 1314-1319.
- 540 Estravis, M., S. Rincon and P. Perez, 2012 Cdc42 regulation of polarized traffic in fission yeast. *Commun*
541 *Integr Biol* 5: 370-373.
- 542 Estravis, M., S. A. Rincon, B. Santos and P. Perez, 2011 Cdc42 regulates multiple membrane traffic events
543 in fission yeast. *Traffic* 12: 1744-1758.
- 544 Frigault, M. M., J. Lacoste, J. L. Swift and C. M. Brown, 2009 Live-cell microscopy - tips and tools. *J Cell Sci*
545 122: 753-767.
- 546 Hachet, O., and V. Simanis, 2008 Mid1p/anillin and the septation initiation network orchestrate
547 contractile ring assembly for cytokinesis. *Genes Dev* 22: 3205-3216.
- 548 Harris, K. P., and U. Tepass, 2010 Cdc42 and vesicle trafficking in polarized cells. *Traffic* 11: 1272-1279.

- 549 Hirota, K., K. Tanaka, K. Ohta and M. Yamamoto, 2003 Gef1p and Scd1p, the Two GDP-GTP exchange
550 factors for Cdc42p, form a ring structure that shrinks during cytokinesis in *Schizosaccharomyces*
551 *pombe*. *Mol Biol Cell* 14: 3617-3627.
- 552 Jin, Q. W., M. Zhou, A. Bimbo, M. K. Balasubramanian and D. McCollum, 2006 A role for the septation
553 initiation network in septum assembly revealed by genetic analysis of *sid2-250* suppressors.
554 *Genetics* 172: 2101-2112.
- 555 Johnson, A. E., D. McCollum and K. L. Gould, 2012 Polar opposites: Fine-tuning cytokinesis through SIN
556 asymmetry. *Cytoskeleton (Hoboken)* 69: 686-699.
- 557 Johnson, D. I., 1999 Cdc42: An essential Rho-type GTPase controlling eukaryotic cell polarity.
558 *Microbiology and molecular biology reviews : MMBR* 63: 54-105.
- 559 Kelly, F. D., and P. Nurse, 2011 Spatial control of Cdc42 activation determines cell width in fission yeast.
560 *Mol Biol Cell* 22: 3801-3811.
- 561 Laporte, D., V. C. Coffman, I. J. Lee and J. Q. Wu, 2011 Assembly and architecture of precursor nodes
562 during fission yeast cytokinesis. *J Cell Biol* 192: 1005-1021.
- 563 Martin, S. G., S. A. Rincon, R. Basu, P. Perez and F. Chang, 2007 Regulation of the formin for3p by *cdc42p*
564 and *bud6p*. *Molecular biology of the cell* 18: 4155-4167.
- 565 McDonald, N. A., A. L. Lind, S. E. Smith, R. Li and K. L. Gould, 2017 Nanoscale architecture of the
566 *Schizosaccharomyces pombe* contractile ring. *Elife* 6.
- 567 McDonald, N. A., C. W. Vander Kooi, M. D. Ohi and K. L. Gould, 2015 Oligomerization but Not Membrane
568 Bending Underlies the Function of Certain F-BAR Proteins in Cell Motility and Cytokinesis. *Dev*
569 *Cell* 35: 725-736.
- 570 Miller, P. J., and D. I. Johnson, 1994 Cdc42p GTPase is involved in controlling polarized cell growth in
571 *Schizosaccharomyces pombe*. *Mol Cell Biol* 14: 1075-1083.
- 572 Moreno, S., A. Klar and P. Nurse, 1991 Molecular genetic analysis of fission yeast *Schizosaccharomyces*
573 *pombe*. *Methods in enzymology* 194: 795-823.
- 574 Onwubiko, U. N., P. J. Mlynarczyk, B. Wei, J. Habiyaemye, A. Clack *et al.*, 2019 A Cdc42 GEF, Gef1,
575 through endocytosis organizes F-BAR Cdc15 along the actomyosin ring and promotes concentric
576 furrowing. *J Cell Sci*.
- 577 Paoletti, A., and F. Chang, 2000 Analysis of *mid1p*, a protein required for placement of the cell division
578 site, reveals a link between the nucleus and the cell surface in fission yeast. *Mol Biol Cell* 11:
579 2757-2773.
- 580 Ren, L., A. H. Willet, R. H. Roberts-Galbraith, N. A. McDonald, A. Feoktistova *et al.*, 2015 The Cdc15 and
581 Imp2 SH3 domains cooperatively scaffold a network of proteins that redundantly ensure
582 efficient cell division in fission yeast. *Mol Biol Cell* 26: 256-269.
- 583 Roberts-Galbraith, R. H., J. S. Chen, J. Wang and K. L. Gould, 2009 The SH3 domains of two PCH family
584 members cooperate in assembly of the *Schizosaccharomyces pombe* contractile ring. *J Cell Biol*
585 184: 113-127.
- 586 Roberts-Galbraith, R. H., and K. L. Gould, 2008 Stepping into the ring: the SIN takes on contractile ring
587 assembly. *Genes Dev* 22: 3082-3088.
- 588 Roberts-Galbraith, R. H., M. D. Ohi, B. A. Ballif, J. S. Chen, I. McLeod *et al.*, 2010 Dephosphorylation of F-
589 BAR protein Cdc15 modulates its conformation and stimulates its scaffolding activity at the cell
590 division site. *Mol Cell* 39: 86-99.
- 591 Schneider, C. A., W. S. Rasband and K. W. Eliceiri, 2012 NIH Image to ImageJ: 25 years of image analysis.
592 *Nat Methods* 9: 671-675.
- 593 Simanis, V., 2015 *Pombe's* thirteen - control of fission yeast cell division by the septation initiation
594 network. *J Cell Sci* 128: 1465-1474.
- 595 Tatebe, H., K. Nakano, R. Maximo and K. Shiozaki, 2008 Pom1 DYRK regulates localization of the Rga4
596 GAP to ensure bipolar activation of Cdc42 in fission yeast. *Current biology : CB* 18: 322-330.

- 597 Tay, Y. D., M. Leda, A. B. Goryachev and K. E. Sawin, 2018 Local and global Cdc42 guanine nucleotide
598 exchange factors for fission yeast cell polarity are coordinated by microtubules and the Tea1-
599 Tea4-Pom1 axis. *J Cell Sci* 131.
- 600 Wang, N., I. J. Lee, G. Rask and J. Q. Wu, 2016 Roles of the TRAPP-II Complex and the Exocyst in
601 Membrane Deposition during Fission Yeast Cytokinesis. *PLoS Biol* 14: e1002437.
- 602 Wei, B., B. S. Hercyk, J. Habiyaremye and M. Das, 2017 Spatiotemporal Analysis of Cytokinetic Events in
603 Fission Yeast. *J Vis Exp*.
- 604 Wei, B., B. S. Hercyk, N. Mattson, A. Mohammadi, J. Rich *et al.*, 2016 Unique Spatiotemporal Activation
605 Pattern of Cdc42 by Gef1 and Scd1 Promotes Different Events during Cytokinesis. *Mol Biol Cell*.
- 606 Wu, J. Q., J. R. Kuhn, D. R. Kovar and T. D. Pollard, 2003 Spatial and temporal pathway for assembly and
607 constriction of the contractile ring in fission yeast cytokinesis. *Dev Cell* 5: 723-734.
- 608 Yonetani, A., and F. Chang, 2010 Regulation of cytokinesis by the formin cdc12p. *Curr Biol* 20: 561-566.
- 609



Supplemental Figure 1. Precocious Cdc42 activation at the division site in *cdc15-27A* cells is *gef1*-dependent. Quantification of Cdc42 activation at the division site from time lapse images the indicated genotypes expressing CRIB-3xGFP and Sad1-mCherry. ****, $p < 0.001$, *, $p < 0.05$, ns=not significant, one-way ANOVA with Tukey's multiple comparisons post hoc test.



Supplemental Figure 2. Gef1 localization is not impaired by loss of *hob3+*. Inverted medial plane images showing Gef1-mNG localization in the indicated genotypes. Scale bar represents 5 μ m.

Table S1. Strains list.		
Strain	Genotype	Source
PN567	<i>h+ ade6-704 leu1-32 ura4-D18</i>	Paul Nurse
YMD926	<i>Gef1-mNeonGreen:kanMX Rlc1-tdTomato NATr Sad1-mCherry:kanMX ade6 leu1-32 ura4-D18</i>	This study
FC2126	<i>pREP42:cdc12ΔC-GFP:ura4+ ade6-M216 leu1-32 ura4-D18 his7+</i>	(YONETANI AND CHANG 2010)
YMD1054	<i>pREP42:cdc12ΔC-GFP:ura4+ Gef1-tdTomato:kanMX ade6 leu1-32 ura4-D18</i>	This study
KGY1105	<i>sid2-250 ade6-M21X ura4-D18 leu1-32</i>	(BALASUBRAMANIAN <i>et al.</i> 1998)
KGY2090	<i>plo1-25</i>	(BAHLER <i>et al.</i> 1998)
YMD872	<i>Δmid1::ura4+ Gef1-3xYFP:kanMX ade6 leu1-32 ura4-D18</i>	This study
YMD844	<i>plo1-1 Gef1-3xYFP:kanMX ade6 leu1-32 ura4-D18</i>	This study
YMD847	<i>sid2-250 Gef1-3xYFP:kanMX ade6-M21X ura4-D18 leu1-32</i>	This study
YMD952	<i>plo1-25 Gef1-mNeonGreen:kanMX Rlc1-tdTomato NATr Sad1-mCherry:kanMX ade6 leu1-32 ura4-D18</i>	This study
YMD954	<i>sid2-250 Gef1-mNeonGreen:kanMX Rlc1-tdTomato NATr Sad1-mCherry:kanMX ade6 leu1-32 ura4-D18</i>	This study
YMD978	<i>mid1Δ Gef1-mNeonGreen:kanMX Rlc1-tdTomato NATr Sad1-mCherry:kanMX ade6-M21X ura4-D18 leu1-32</i>	This study
YMD317	<i>CRIB-3xGFP:ura4+ Rlc1-tdTomato:NATr Sad1-mCherry:kanMX ade6-M21X leu1-32 ura4-D18 his7+</i>	(WEI <i>et al.</i> 2016)
YMD488	<i>Δgef1::ura4+ CRIB-3xGFP:ura4+ Rlc1-tdTomato:NATr Sad1-mCherry:kanMX ade6 leu1-32 ura4-D18 his7+</i>	(WEI <i>et al.</i> 2016)
YMD133	<i>Cdc15-GFP:kanMX6 sad1-mCherry:kanMX ade6-M21X leu1-32 ura4-D18</i>	(WEI <i>et al.</i> 2016)
YMD973	<i>cdc15ΔSH3-GFP:kanMX Gef1-tdTomato:kanMX Sad1-mCherry:kanMX ade6-M21X ura4-D18 leu1-32</i>	This study
YMD991	<i>Cdc15-GFP:kanMX Gef1-tdTomato:kanMX Sad1-mCherry:kanMX ade6-M21X ura4-D18 leu1-32</i>	This study
YMD929	<i>gef1S112A:ura4+ kanMX ade6-M210 ura4-D18 leu1-32</i>	This study
YMD710	<i>Δgef1::ura4+ ura4-D18 leu1-32</i>	This study

KGY7051	<i>cdc15ΔSH3 ade6-M210 leu1-34 ura4-D18</i>	(ROBERTS-GALBRAITH <i>et al.</i> 2009)
KGY10303	<i>cdc15-27A ade6-M21X leu1-32 ura4-D18</i>	(ROBERTS-GALBRAITH <i>et al.</i> 2010)
KGY9723	<i>cdc15-27D ade6-M21X leu1-32 ura4-D18</i>	(ROBERTS-GALBRAITH <i>et al.</i> 2010)
KGY10307	<i>cdc15-27A-GFP:kanMX ade6-M21X leu1-32 ura4-D18</i>	(ROBERTS-GALBRAITH <i>et al.</i> 2010)
YMD1155	<i>Cdc15-GFP:kanMX Gef1-tdTomato:kanMX ade6-M21X leu1-32 ura4-D18</i>	This study
YMD1145	<i>cdc15-27A-GFP:kanMX Gef1-tdTomato:kanMX ade6-M21X leu1-32 ura4-D18</i>	This study
YMD1243	<i>Cdc15-GFP:kanMX Scd1-tdTomato:kanMX ade6-M21X leu1-32 ura4-D18</i>	This study
YMD1212	<i>cdc15-27A-GFP:kanMX Scd1-tdTomato:kanMX ade6-M21X leu1-32 ura4-D18</i>	This study
YMD121	<i>CRIB-3xGFP:ura4+ Sad1-mCherry:kanMX ade6-M21X leu1-32 ura4-D18</i>	This study
YMD1143	<i>cdc15-27A CRIB-3xGFP:ura4+ Sad1-mCherry:kanMX ade6-M21X leu1-32 ura4-D18</i>	This study
YMD1242	<i>Δgef1::ura4+ cdc15-27A CRIB-3xGFP:ura4+ Sad1-mCherry:kanMX ade6-M21X leu1-32 ura4-D18</i>	This study
YMD1097	<i>Δhob3::kanMX Gef1-mNeonGreen:kanMX ade6-M21X leu1-32 ura4-D18</i>	This study

References

- Bahler, J., A. B. Steever, S. Wheatley, Y. Wang, J. R. Pringle *et al.*, 1998 Role of polo kinase and Mid1p in determining the site of cell division in fission yeast. *J Cell Biol* 143: 1603-1616.
- Balasubramanian, M. K., D. McCollum, L. Chang, K. C. Wong, N. I. Naqvi *et al.*, 1998 Isolation and characterization of new fission yeast cytokinesis mutants. *Genetics* 149: 1265-1275.
- Roberts-Galbraith, R. H., J. S. Chen, J. Wang and K. L. Gould, 2009 The SH3 domains of two PCH family members cooperate in assembly of the *Schizosaccharomyces pombe* contractile ring. *J Cell Biol* 184: 113-127.
- Roberts-Galbraith, R. H., M. D. Ohi, B. A. Ballif, J. S. Chen, I. McLeod *et al.*, 2010 Dephosphorylation of F-BAR protein Cdc15 modulates its conformation and stimulates its scaffolding activity at the cell division site. *Mol Cell* 39: 86-99.
- Wei, B., B. S. Hercyk, N. Mattson, A. Mohammadi, J. Rich *et al.*, 2016 Unique Spatiotemporal Activation Pattern of Cdc42 by Gef1 and Scd1 Promotes Different Events during Cytokinesis. *Mol Biol Cell*.

Yonetani, A., and F. Chang, 2010 Regulation of cytokinesis by the formin cdc12p. *Curr Biol* 20: 561-566.